AFRL-AFOSR-VA-TR-2019-0245

# Reconfigurable, High-Frequency Circuit Components using Phase Change Materials

Hjalti Sigmarsson
UNIVERSITY OF OKLAHOMA

07/26/2019
Final Report

**DISTRIBUTION A: Distribution approved for public release.**

Air Force Research Laboratory
AF Office Of Scientific Research (AFOSR)/ RTA1
Arlington, Virginia 22203
Air Force Materiel Command

# REPORT DOCUMENTATION PAGE

*Form Approved*
*OMB No. 0704-0188*



**1. REPORT DATE** *(DD-MM-YYYY)*
16-08-2019

**2. REPORT TYPE**
Final Performance

**3. DATES COVERED** *(From - To)*
01 May 2015 to 30 Apr 2019

**4. TITLE AND SUBTITLE**
Reconfigurable, High-Frequency Circuit Components using Phase Change Materials

**5a. CONTRACT NUMBER**

**5b. GRANT NUMBER**
FA9550-15-1-0136

**5c. PROGRAM ELEMENT NUMBER**
61102F

**6. AUTHOR(S)**
Hjalti Sigmarsson

**5d. PROJECT NUMBER**

**5e. TASK NUMBER**

**5f. WORK UNIT NUMBER**

**7. PERFORMING ORGANIZATION NAME(S) AND ADDRESS(ES)**
UNIVERSITY OF OKLAHOMA
201 David L. Boren Blvd Suite 150
Norman, OK 73019-5300 US

**8. PERFORMING ORGANIZATION REPORT NUMBER**

**9. SPONSORING/MONITORING AGENCY NAME(S) AND ADDRESS(ES)**
AF Office of Scientific Research
875 N. Randolph St. Room 3112
Arlington, VA 22203

**10. SPONSOR/MONITOR'S ACRONYM(S)**
AFRL/AFOSR RTA1

**11. SPONSOR/MONITOR'S REPORT NUMBER(S)**
AFRL-AFOSR-VA-TR-2019-0245

**12. DISTRIBUTION/AVAILABILITY STATEMENT**
A DISTRIBUTION UNLIMITED: PB Public Release

**13. SUPPLEMENTARY NOTES**

**14. ABSTRACT**
Germanium telluride (GeTe) phase-changing material (PCM) was grown for the first time using a pulsed electron deposition (PED) tool. This includes: the demonstration of various film thicknesses, the determination of GeTe growth conditions, the characterization of GeTe growth rates, and an investigation of the deposited film quality. The detailed study on the growth of GeTe using PED was published in a journal. Second paper in preparation with details on activation of PED-grown GeTe. Switches and tunable filters have been designed using GeTe PCM. This work will continue through the year and further publications are expected.

**15. SUBJECT TERMS**
effective quality factor, electronically tunable substrate materials, varactor, reconfigurable substrate, reconfigurable devices, high-Q absorptive bandstop filters, Parylene, phase changing material

| 16. SECURITY CLASSIFICATION OF: a. REPORT | b. ABSTRACT | c. THIS PAGE | 17. LIMITATION OF ABSTRACT | 18. NUMBER OF PAGES |
|---|---|---|---|---|
| Unclassified | Unclassified | Unclassified | UU | |

**19a. NAME OF RESPONSIBLE PERSON**
POKINES, BRETT

**19b. TELEPHONE NUMBER** *(Include area code)*
703-588-1772

Final Performance Report

Air Force Young Investigator Research Program

# Reconfigurable, High-Frequency Circuit Components using Phase Change Materials

**Due July 30, 2019**

**Dr. Hjalti H. Sigmarsson**
**Radar Innovations Laboratory**
**3190 Monitor Ave.**
**Norman, OK 73019**
**Phone: (405) 325-2971, Fax: (405) 325-7066**
**h.sigmarsson@ou.edu**

## TABLE OF CONTENTS

# 1 PROJECT GOALS

The purpose of this project was to investigate the use of phase-change materials (PCMs) to create a wide range of reconfigurable high-frequency component building blocks. These included varactors, switches, and artificial dielectrics. An important part of this effort was the development of processing parameters for depositing PCMs using pulsed electron deposition (PED).

An alternative growth method was also investigated in parallel with the PED growth. This method consisted of creating a liquid suspension that contains PCM particles and then using a commercial 3D printer to selectively deposit PCM pockets. This allows an inexpensive and rapid method for prototyping switches, phase shifters, and other reconfigurable electronics.

The ultimate project goal was to create an electronically tunable substrate material that allows for tuning of both frequency and loss of a resonator by controlling both the tank capacitance and the effective Q. This new artificial substrate material was to be used to demonstrate an extension of the available tuning range of high-Q absorptive band-stop filters. For this application, precise amplitude matching of parallel signal paths is required for optimum signal cancellation.

Overall, the outcome of the project was thorough guidelines on how to grow and activate Germanium Telluride (GeTe) using the PED tool.

# 2 MATERIAL GROWTH

The first task that was addressed was the growth of GeTe using the PED in the University Cleanroom. To evaluate the qualifications of the PED method, thin films of GeTe are grown and investigated by contemplating the surface morphology and the material composition. High-quality GeTe thin films with thicknesses from 30 to 200 nm, were successfully grown on top of silicon wafers at room temperature to demonstrate the ability of PED. To optimize the growth procedure, several growth parameters were thoroughly investigated, including background pressure, pulse energy, and growth temperature. A series of material characterization methods were adopted to study the GeTe material quality after the growth. These methods include field emission scanning electron microscope (FESEM), energy-dispersive X-ray spectroscopy (EDX), X-ray diffraction (XRD), and thickness profilometer.

## 2.1 MATERIAL CHARACTERIZATION

The characterization started with thickness measurement using a step profiler from KLA-Tencor. Surface morphology and composition of the films were observed with a high-resolution scanning electron microscope (Zeiss NEON 40 EsB, High-Resolution FEG-SEM with FIB). A Hall measurement system (Ecopia HMS 5000) in Van der Pauw four-point probe configuration was used to determine the polarity of the charge carrier, resistivity, mobility, Hall coefficients, carrier concentration, and magnetoresistance.

The crystallographic information of the deposited films was extracted by X-ray diffraction carried out by a diffractometer (Rigaku Ultima IV). The X-ray source (40 kV, 44 mA) generates a Cu-Kα radiation (1.54059 Å) and the diffracted beam is collected with a scintillation detector. Finally, the composition of the different layers was probed with Energy Dispersive X-ray (EDX) microanalysis.

All the results of the early material characterization were included in last year's annual report. During the switch testing, issues were detected with the film quality. Therefore, the fabrication process was revised. This new characterization and processing are included in the next section.

## 2.2 Material Deposition

### *2.2.1 PCM*

A first-time demonstration of using a novel method for growing GeTe thin films is reported. This growth method is called pulsed electron-beam deposition (PED). The ablation mechanism in PED is similar to PLD, where the laser beam is replaced by concentrated electron beam. While PLD suffers from optical shielding of the target surface, the electron beam in PED is not reflected by the plasma, which results in improved efficiency. Also, there is no need for large, expensive excimer lasers and optical setups that are necessary for PLD. To demonstrate the PED capabilities, GeTe thin film, the most motivating PCM in the high-frequency applications is targeted. The primary motivation of this study is to demonstrate the advantages of utilizing PED method for growing complex composite thin-film materials.

**2016:**

A 1” diameter sputtering target was acquired from American Elements. The distance between the gun-tip and the target is approximately 2 mm. Substrate holder was 6 cm vertically apart from the target. The substrate holder can accommodate four 1 cm x 1 cm samples in a single run. The phase of the as-grown films is amorphous. Heating the films at 300°C for 5 minutes on a hot plate changes them into crystalline phase.

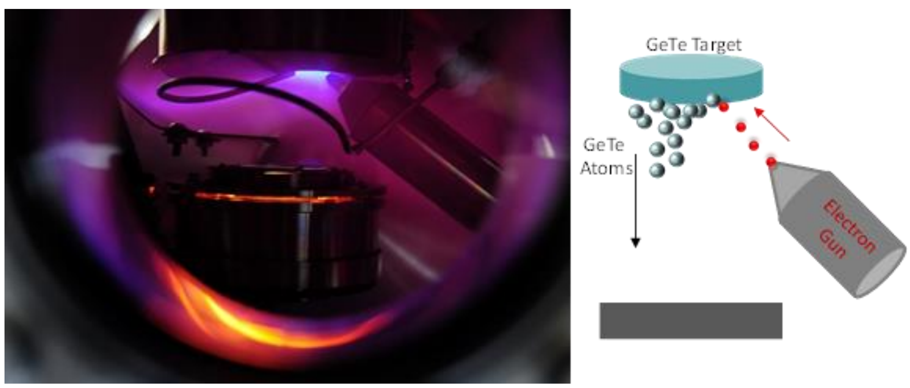


Figure 1. Pulsed Electron-beam Deposition (PED) in operation on the left along with a visualization on the right.

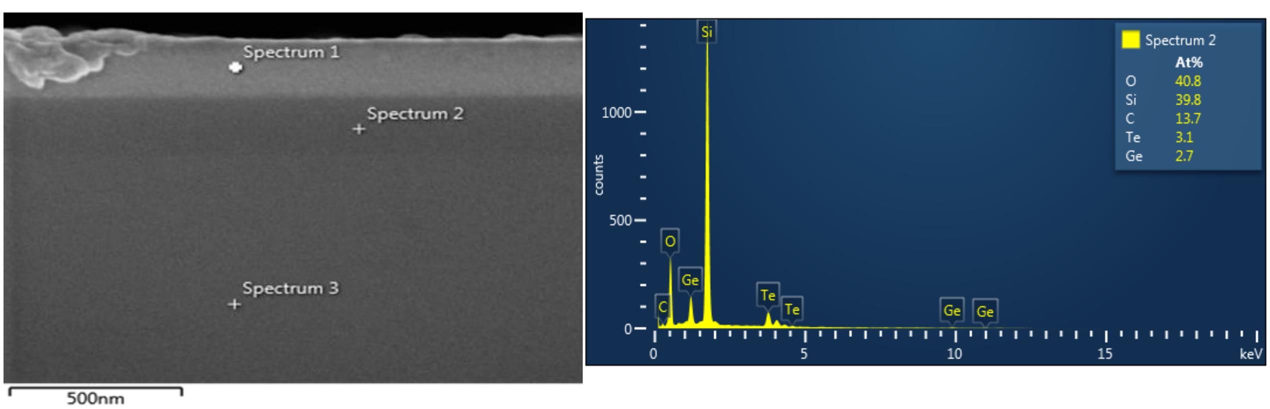


Figure 2. Cross section SEM view of GeTe thin film and Energy Dispersive X-ray spectra of germanium telluride

## 2017:

During the switch testing, issues were detected with the film quality. Therefore, the fabrication process was revised. The initial procedure was revised in this last year and the PED tool has undergone several changes. The growth rate was found to be highly dependent on the electron gun cleanliness. Material was found be building up around the electron gun tip and it was resulting in reducing film thicknesses as a function of time. A new method was developed for cleaning the electron gun using hydrochloric acid. This process adds to the post cleaning time. Other changes include a new sample holder was machined to bring the substrates closer to the target for improved growth rates, and the integration of a crystal growth rate measurement system to allow for in-situ growth monitoring.

a) b)

Figure 3. PED tool modifications. a) Extended sample holder for improving the material growth rate, and b) growth rate measurement system for improved film thickness control.

## 2018:

Firstly, the chamber of PED deposition was modified by replacing the butterfly valve with a turbo valve which gives the operator much better control on the chamber pressure. Also, a shutter was added to chamber which is essential for material growth, as during the set-up parameters for deposition, the chamber conditions are not stable and the ablated material's atom/molecules do not have the desirable quality, it covers the substrate surface. Moreover, a growth rate measurement system for improved film thickness control was added to the system.

The previous year PED deposition and characterization of GeTe continued, we found out that deposition at room temperature has the highest growth rate, while high-temperature growth has not affected the crystal quality and all thin films of GeTe are amorphous as grown and need post heat treatment for crystallization. The other parameter affects the growth rate is the pulse's voltage produced by PED, we know it as pulse power. The results of both temperature and voltage on the growth rate are illustrated in Figure 4.

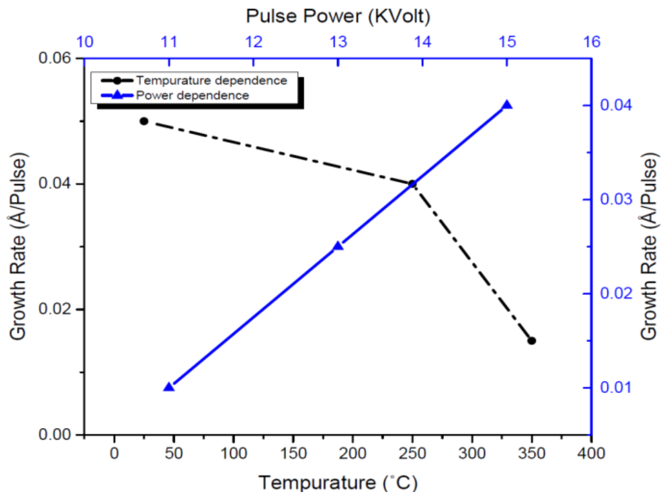


Figure 4. Growth rate dependence to applied power of PED and substrate temperature.

Another parameter can control the film quality is the distance between target and substrate. Although the closer substrate to the target has the higher growth rate, the films deposited at a longer distance have much better quality in terms of surface smoothness. Pressure is the other constraint affects the film quality. Figure 5 shows SEM top view of 5 GeTe thin films deposited at a different pressure. Lower the pressure better film quality, however, it cannot be decreased more since it ended up to an error in PED system because lower pressures result in suspension of gun operation causing “missing pulse”.

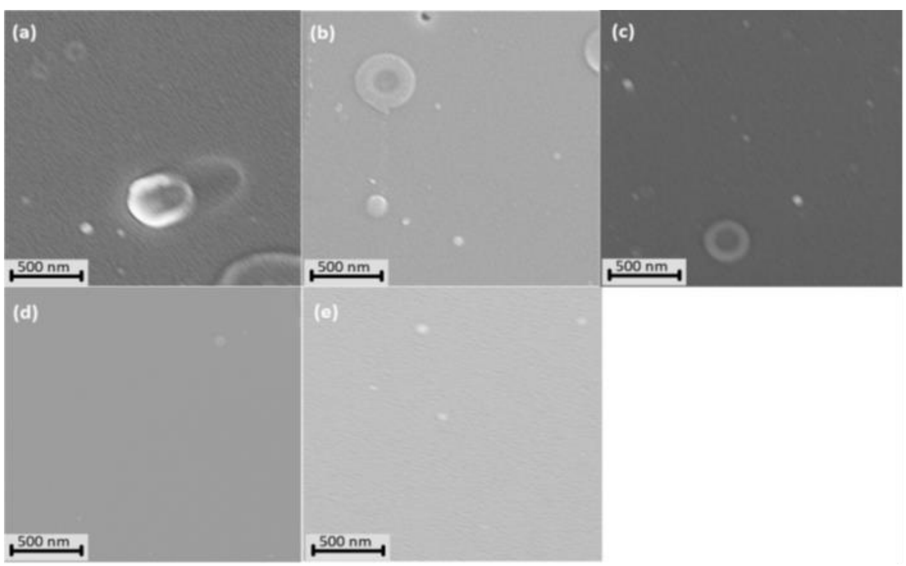


Figure 5. Top SEM view of GeTe thin films deposited by PED in various background pressure: (a)7.5mTorr, (b) 6.8mTorr, (c) 5.5mTorr, (d) 5.5mTorr and (e) 4.5mTorr; and two target and substrate distances: (a-c) at shorter distance, and (d-e) at longer distance.

## 2019:

Although higher beam energy results in a higher growth rate and enhanced throughput, the surface morphology is determined by the energy that the target material requires for evaporation. If the applied voltage is lower than the optimum, lead to low growth rate due to the lack of energy to ablate the material. This was found when 11 and 13 kV potentials were applied to the PED gun. To increase the growth speed, the voltage was increased to 15 kV, which resulted in a growth rate of 0.04 Å/pulse or 1.2 nm/min. This is a reasonable rate for GeTe deposition compared to PLD. Raising the voltage to 17 kV resulted in a higher growth rate, but poor film quality, in terms of number and the size of particulates formed on the surface. Nevertheless, the size and number of these particulates drop when the substrate is placed at the end of the plume range. This is because the optimal target-to-substrate distance is adjacent to the plume range. The plume range is an important E-beam parameter during the growth. The key features that define the plume range are the applied PED voltage and the target-to-substrate distance. In our experiments, three different target-to-substrate distances were tested. The highest distance from the target that the chamber allows is 8 cm. Two extender substrate holders were used to grow thin films at 3 and 5 cm as well as 8 cm. The top view morphology results of 3, 5, and 8 cm are shown in Figure 6 (a) to (c), respectively. The average growth rate has a linear and negative dependency on the target to substrate distance. Figure 6 shows that, by decreasing the target substrate distance, some irregular particulates are formed on the deposited films. Although closer target resulted in a higher growth rate, the surface roughness was increased, and subsequently, the film quality reduced drastically. Lower the target-to-substrate distance resulted in larger particulates' sizes and densities. The arithmetical mean deviation surface roughness, $R_a$, was calculated from the measured height profile captured using a KLA stylus profilometer. The larger the distance, the smoother the surface. By increasing the target-to-substrate distance, a drastic reduction in the number and size of the particulates in the deposited film were observed, and the smoother surface was obtained.

Since the 8 cm distance resulted in the best surface morphology, and it is the largest distance that the chamber allows, the rest of the experiments were conducted at this distance. A higher PEBS potential (17 kV) was tested to confirm that 15 kV is the optimum PEBS voltage. Lower surface roughness results in higher performance of PCM in high-frequency applications. The purpose is to achieve smooth film with no particulates larger than 200 nm, and with less than 1% of particulates covering the entire surface. The surface morphology of the as-deposited GeTe films, grown at 15 and 17 kV are shown in Figure 7 (a) and (b), respectively. The results confirm that the 15 kV satisfies the desired requirements, and therefore it is the potential used for the rest of the experiments

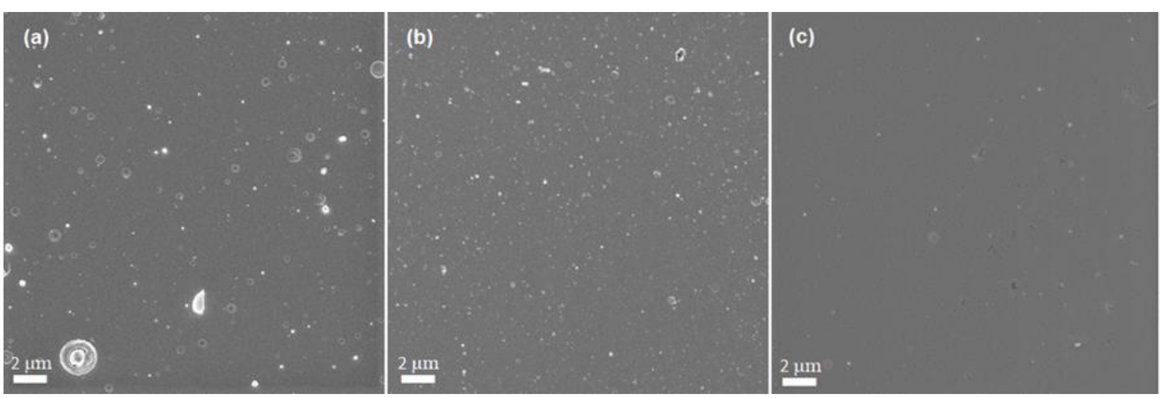


Figure 6. Top SEM view of GeTe thin films deposited at (a) 3 cm (b) 5 cm and (c) 8 cm target-to-substrate distances at pressure of 5.5 mTorr and PEBS of 15 kV.

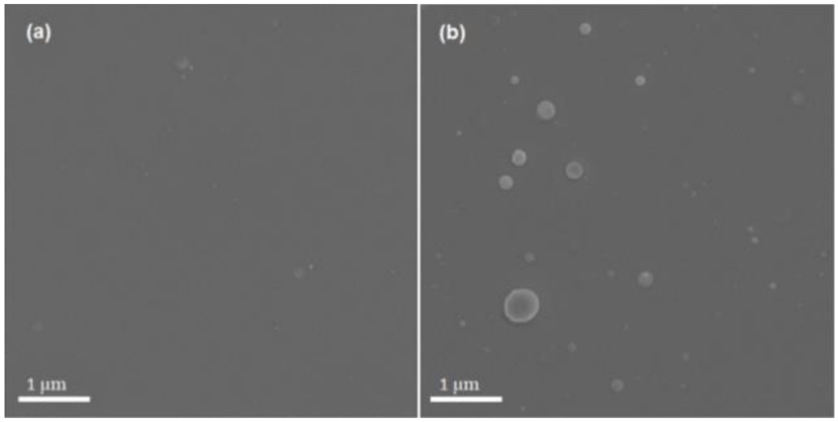


Figure 7. Top SEM view of GeTe thin films deposited at (a) 15 kV and (b) 17 kV PEBS potentials at pressure of 5 mTorr and target-to-substrate distance of 8 cm.

Another challenge in the PCM thin film growth, which determines the sheet resistance, is reaching the proper ratio between material concentrations in the deposited thin film. GeTe (50:50) has the lowest sheet resistance of the GST family of PCM. Previous research on GeTe materials showed that a slight change in the ratio of the elements does not have a considerable variation in the PCM properties. Figure 8 illustrates the impact of the background pressure on the ratio between Ge and Te in the deposited material. Higher pressures result in telluride rich, thin films. This occurs because telluride rich clusters like $GeTe_2$ are formed and present in the plasma. These molecules can be deposited on the substrate at higher pressures. The ratio between elements in the composition of Ge:Te can be controlled by reducing the pressure. Based on the trend of decreasing telluride and increasing germanium, the 2.6 mTorr provides $Ge_{50}Te_{50}$, which is the exact 50:50 stoichiometric composition desired. The error in EDX measurements was 2 Sigma, which means two standard deviations away from the mean in a normal distribution or 95.4% accuracy. To reduce the error, every sample was measured several times on different areas. The variation in the measured elemental ratios is around 0.5%, and the reported values in Figure 8 represent their averages.

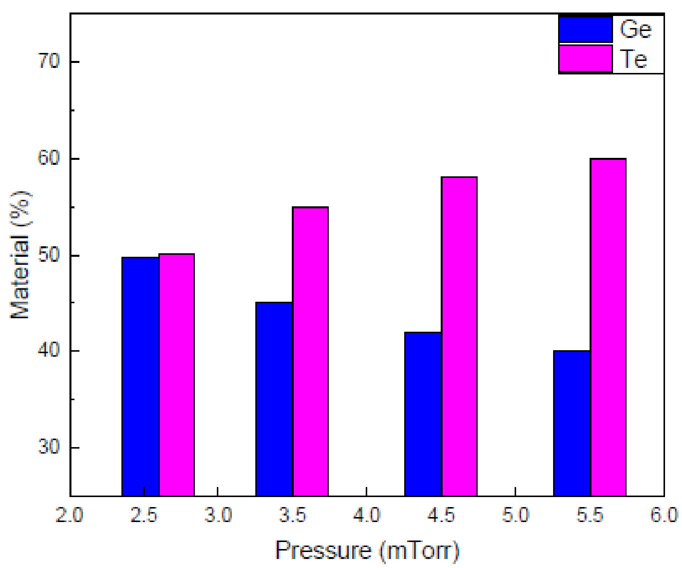


Figure 8. Germanium and Telluride ratio dependence on pressure.

Amorphous and crystalline are two stable phases of PCM at room temperature. Epitaxial growth of materials can be performed at high temperatures to reach single crystalline thin-films material. On the other hand, PVD methods are generally used to deposit PCM thin films at room-temperature. In this study, the growth of the GeTe thin films, using the PED method, was performed at room temperature. Figure 9 shows the XRD pattern for the GeTe thin film as deposited. The broad crest on the three-major crystalline GeTe materials' peaks ((003), (021) and (202)) verifies the amorphous structure of the as-deposited GeTe thin film. Post-annealing methods are commonly used to transform the amorphous as-deposited PCM material to a crystalline state.

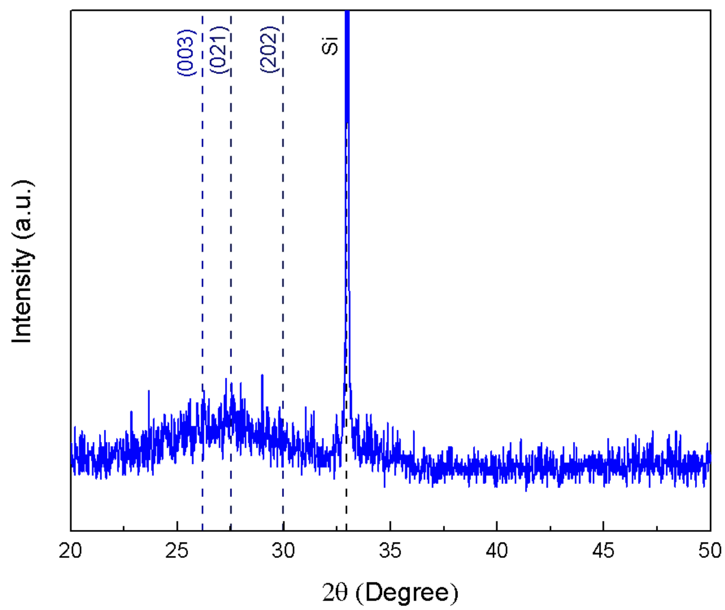


Figure 9. X RD pattern of the as-deposited GeTe film.

### 2.2.2 *Post Thermal Treatment*

Finally, after the growth optimization, FESEM images revealed that the as-grown GeTe films were of high smoothness and uniformity. EDX analysis indicated that the compositions of the GeTe films were pressure dependent. Through the XRD spectrum, it is found that the as-grown GeTe films were amorphous. In order to convert them into crystalline formation, further post-treatment approaches (e.g., annealing). As discussed in [2], in order to have more efficient switching the amorphous deposited GeTe film should transform to crystalline completely, because the phase change by the heater in device happens on a small portion of the PCM layer. So, the normally ON switch is more efficient.  Figure 10 illustrates this concept.

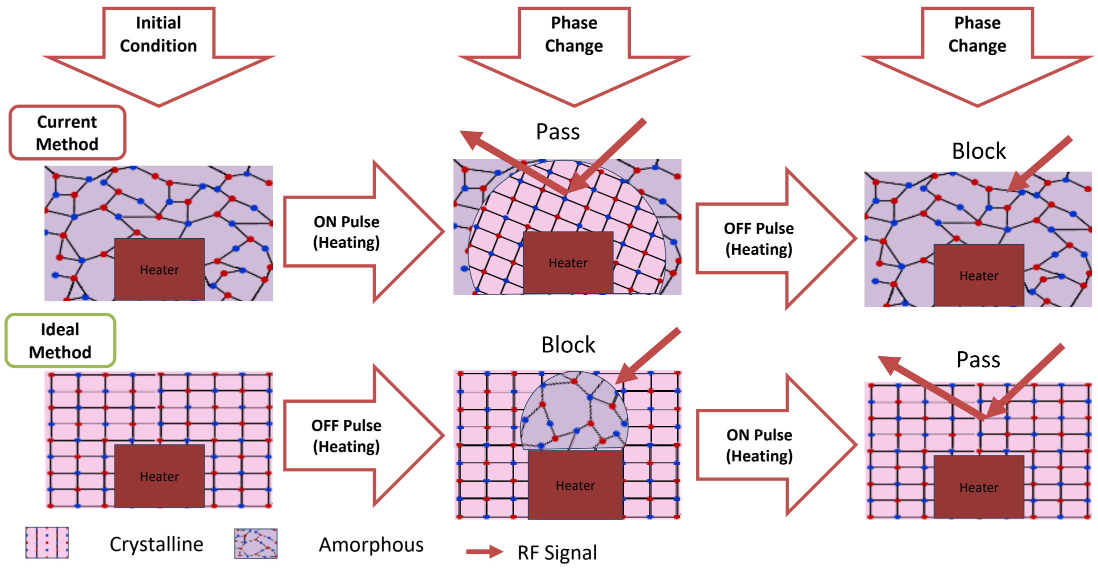


Figure 10. The configuration on the top represents the situation with the current samples, where the initial condition of the film is amorphous and only a small portion of the switch changes phase. The bottom shows a more ideal way, where the starting point is crystalline and activating the channel results in the off state [2].

Several post heat treatments were done under various conditions: temperature, time, and pressure. A variety of different crystalline states were achieved with the best one coming from Growth #10 Run #2 (10-2). The X-Ray diffraction (XRD), which is used to study the crystal structure of the material, was done for the samples to find the best conditions for making GeTe crystalline. Full Width Half Maximum (FWHM) is a factor to indicative of crystal size and strain. The smaller the size the greater the value of FWHM, and the same holds true for the strain. Figure 11 shows the XRD results for thermal annealing of the deposited samples. During the crystallization process, a clear crystalline GeTe peak at 29.98 and/or 26.2 degrees can be achieved.

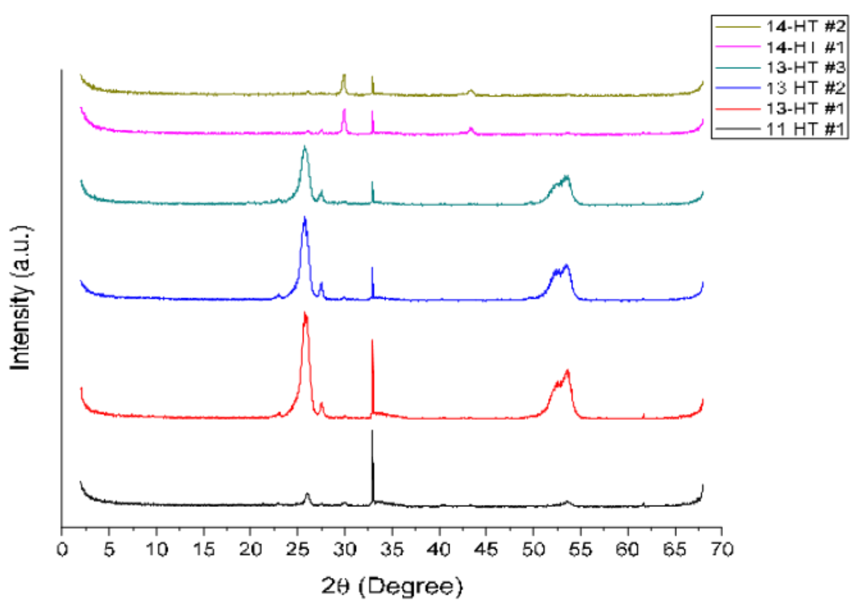


Figure 11. XRD results from different crystallization.

### 2.2.3 Dielectric

$SiO_2$ as a good dielectric material was used for the layer between heater and PCM to provide electrical insulation [1], however, it suffers from low thermal conductivity needed to transfer the generated heat from heater to PCM layer. The best dielectric material with high thermal conductivity is Aluminum Nitride (AlN) [2]. The first tries for depositing AlN by PED was unsuccessful due to its surface roughness [2], as result, the direct heating switch with eliminating dielectric layer was fabricated [2] its results were not satisfactory. After adding the sputtering system to PED chamber, two different sputtering of AlN were tested, RF with AlN target and DC with Al target. The RF sputtering with insulator AlN target throughput was too low and very hard to deposit. 11 runs of DC sputtering with conductor Al target in Ar and N2 gases combinations under various parameters were tested to achieve the best film quality with the best thermal conductivity and highest electrical resistivity. Figure 12 shows the SEM top view of the AlN thin film.

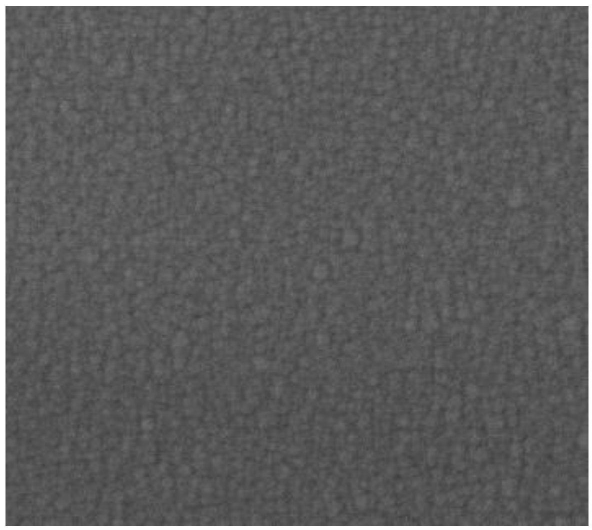

Figure 12. SEM top view of AlN thin film deposited by DC sputtering.

### 2.2.4 Heater

NiCr was used for the heater in previous device fabrications has a low melting point close to GeTe's (1400˚C and 750˚C) that affects the device performance. The best candidates for heater are Molybdenum (Mo) and Tungsten (W) with high melting points, 2900˚C, and 3700˚C, respectively, and low resistivity (53 nΩ-m). The first deposition method was tested for both Mo and W was E-beam deposition. The PR was burnt during deposition since the E-beam chamber becomes very hot. To solve this problem, etching was tested for W. The etchant type, ratio, and etch rate were found after several tests. However, the results were not definite and some residual material remaining in the gaps, this is shown in Figure 13 (a). This resulted in a change in the deposition method to sputtering. As the low resistivity and high quality of W films are obtained using high-temperature deposition, etching is the preferred patterning method for W. Four runs of sputtering W and 10 runs of etching have been done to reach the best results of low resistivity high quality of Tungsten as heater layer. Figure 13 (b) shows the result of the etched W deposited by sputtering.

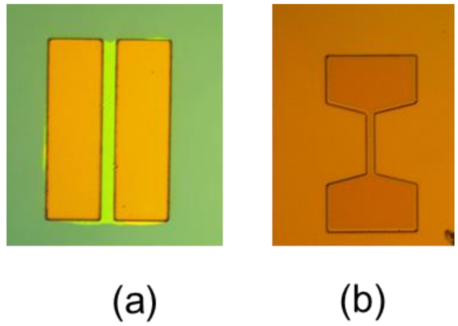


Figure 13. The etch results of W deposited by (a) E-beam and (b) Sputtering.

Tungsten can exist in two forms of an A2 α-W with no metastable and high-resistivity metastable A15 β-W phases. The reported bulk resistivity metastable β-W phase is in the range of 150–350 μΩ.cm; therefore, even small quantities of β-W in the films can result in high film resistivities. Low resistivity tungsten is crucial for the power required for switch actuation. The as-grown tungsten #6 and #7 are fully in β-W phase with high resistivity. Growth #8 is in both β-W and α-W phases, with lower resistivity but still high. Post thermal treatment under different gas types, temperature, time, and pressure was performed to convert all the tungsten to low resistivity α-W. Two of the best results are reported in Figure 14.

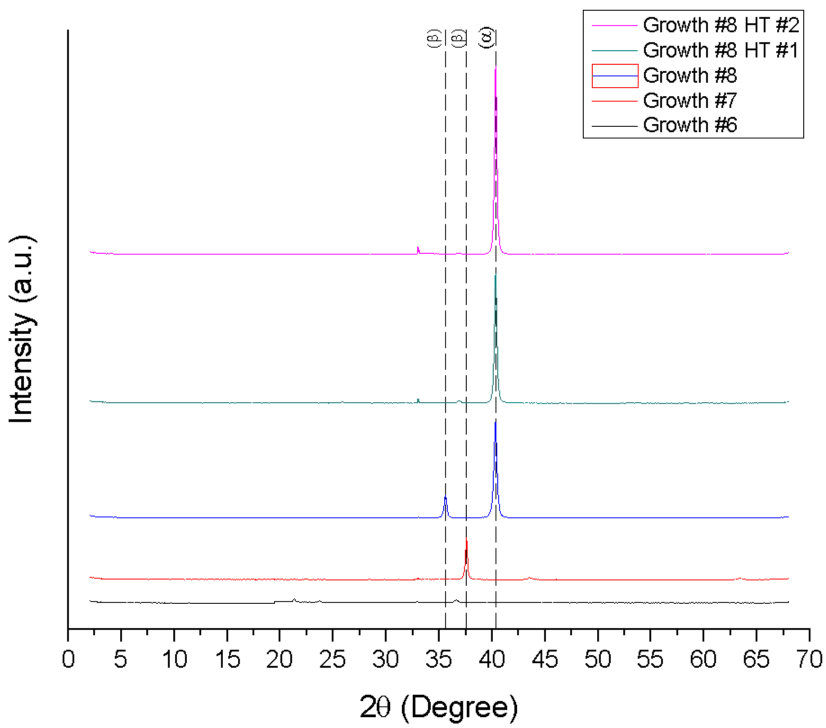


Figure 14. XRD results for three tungsten growth and post thermal annealing.

## 3 ELECTRICAL TESTING

The amorphous phase is a good insulator and the crystalline phase is a good conductor. The resistance of the conductive phase was five orders of magnitude lower than that of insulating phase, which is a huge contrast that is desired for reliable switching application. The average resistances of the amorphous and crystalline phases of GeTe were 130 ± 24 MΩ and 247 ± 70 Ω, respectively. Further details are found in [1].

### 3.1 DEVICE DESIGN

#### *3.1.1 RF Switch*

Two switch designs were selected for fabrication as discussed previously [1]. One design with direct biasing to change the phase of the PCM and one design for the laser heating. These switch designs can be seen in Figure 15 along with the material stack-up for each device. The first design included a NiCr heater to allow for probe-driven heating. The heater was covered by a sputtered $SiO_2$ layer to minimize the impact of the heater on the RF signal path.

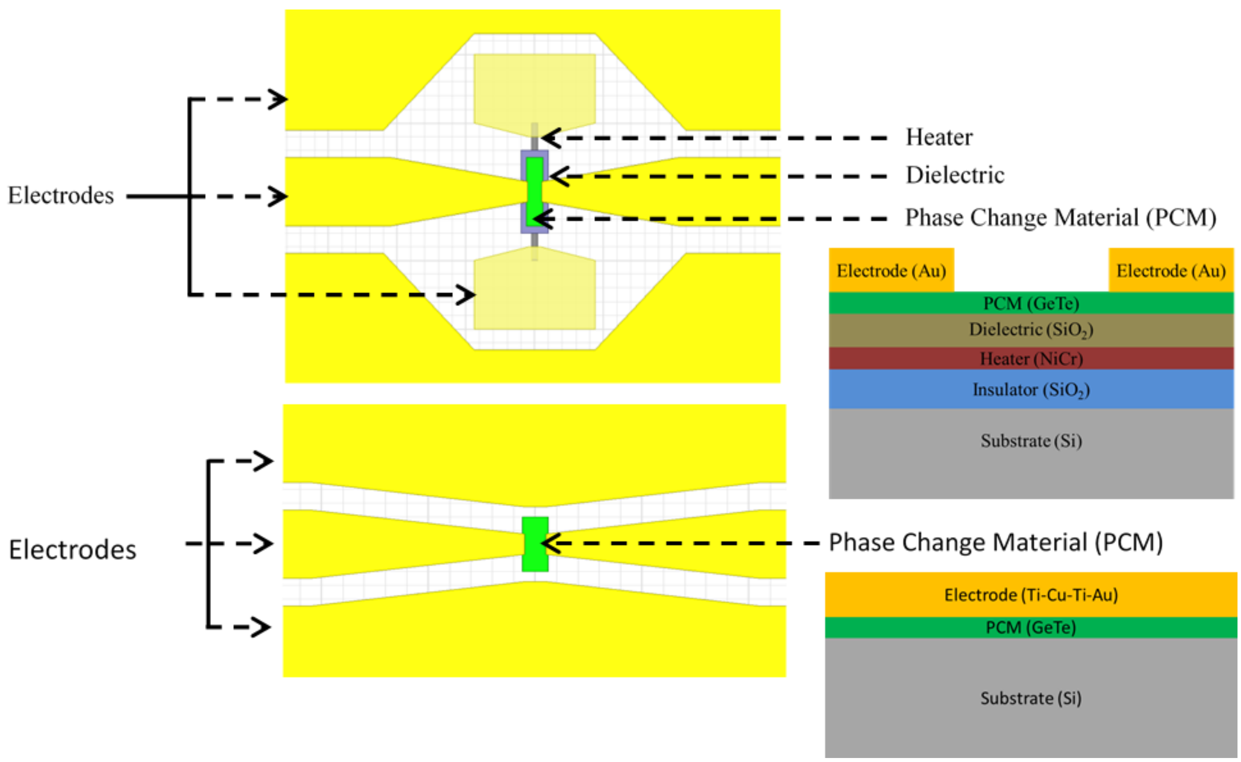


Figure 15. Layout of PCM-based RF switch. (a) Top-view of Design 1, (b) materials stack-up for Design 1, (c) top-view of Design 3, (d) material stack-up for Design 3.

**2018:**

The first device that was designed has some problems, the RF gap was too large and more importantly wider than heater width. This results in the RF signal cannot pass through the PCM due to the heater heats up a narrower portion of PCM than its width. As a result, the phase change occurs in PCM narrower than RF gap. This parameter has a very critical impact on the device performance. So, a new mask with various heater width and RF gap for different switches was designed, in all of them, RF gap is smaller than the heater width. Figure 16 shows the old and new structures of switches. The first design included a W heater to allow for the direct biasing. The heater was covered by a sputtered AlN layer to minimize the impact of the heater on the RF signal path. The second design does not require an insulator as no bias traces are included. The two switch designs, as well as several reference standards, are placed on the designed mask. The standards were included in the fabrication run to establish a baseline for an open-circuited switch and a short-circuited switch by creating lines without any GeTe and lines with Ti-Au-Ti-Cu replacing the GeTe material.

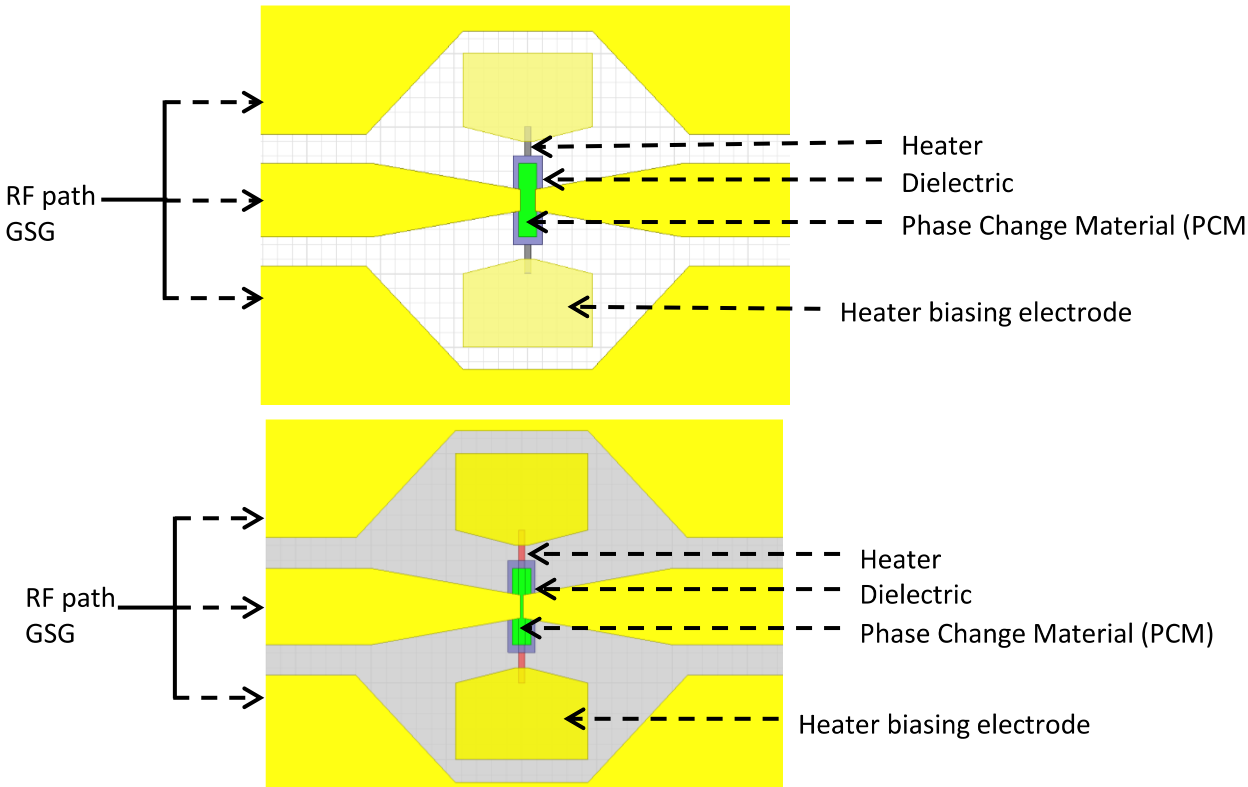


Figure 16. Layout of PCM-based RF switch, old structure on top and new design on bottom.

## 3.2 Device Fabrication

### 2016:

Three fabrication runs were completed with the RF switches. First batch was on $SiO_2$/Si substrate with a positive mask set and lift-off. This process soon revealed its weakness as we deposited thicker (600 nm) layer of metal as electrode. Due to the positive slope of the positive tone photoresist, the sidewalls were connected for thicker deposited layer on top of the photoresist. As a result, subsequent lift-off process was very difficult. Figure 17 shows the results obtained from different steps of the fabrication process of run 1. The edges on the electrode layer after lift-off is not very clean due to higher thickness of this layer. It was Ti-Cu-Ti-Au (15-500-10-100) nm thick and the resist was about 1.2 µm. The tone of the resist is also another reason for not having good edges

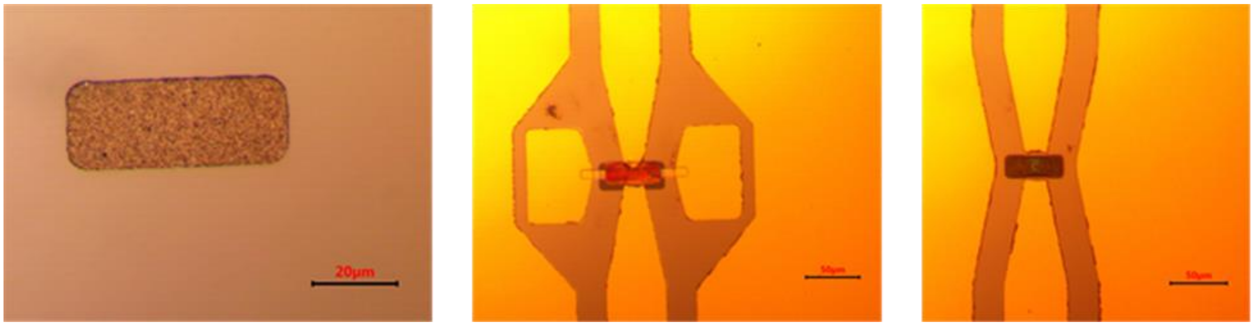


Figure 17. RF switch fabrication run 1

## 2017:

For each fabrication run, the two aforementioned switches were included as well as several reference standards. The standards were included in the fabrication run to establish a baseline for an open-circuited switch and a short-circuited switch by creating lines without any GeTe and lines with Ti-Au-Ti-Cu replacing the GeTe material. The fabricated devices for one of the fabrication runs are shown in Figure 18. To test the consistency of the fabrication, a third fabrication run was completed. The parts built in the third fabrication run were identical to the ones in the second fabrication run

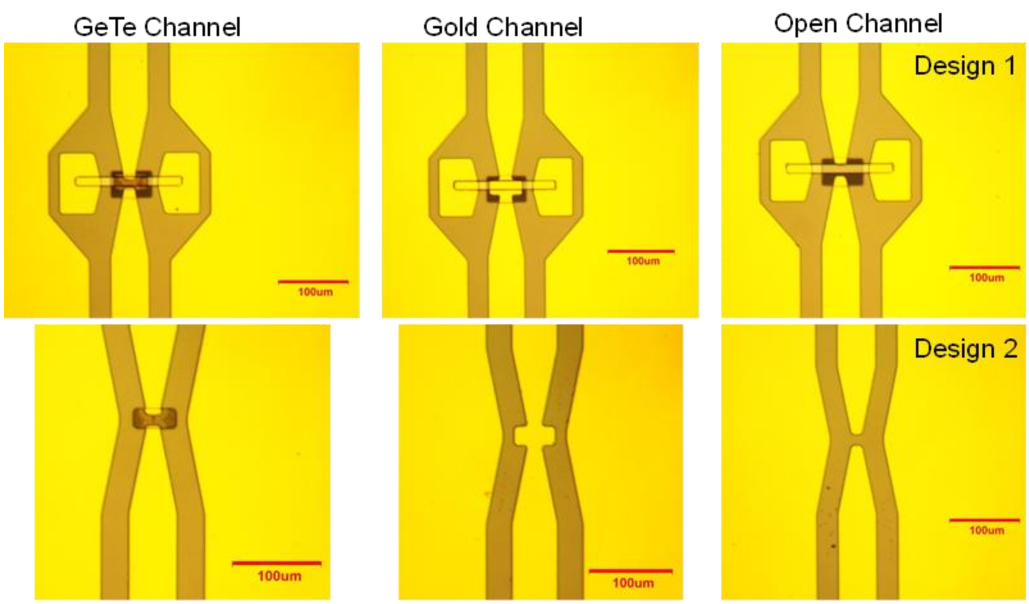


Figure 18. Devices included on the RF switch fabrication runs; left shows the devices with PCM, middle shows the short-circuited reference, and the right shows the open-circuited reference.

## 2018:

Several RF-switch, fabrication runs were completed in this year of the project in continue of the last year fabrications. The initial runs followed the previously reported procedure [2]. All switch fabrication runs used the third mask set from [2].

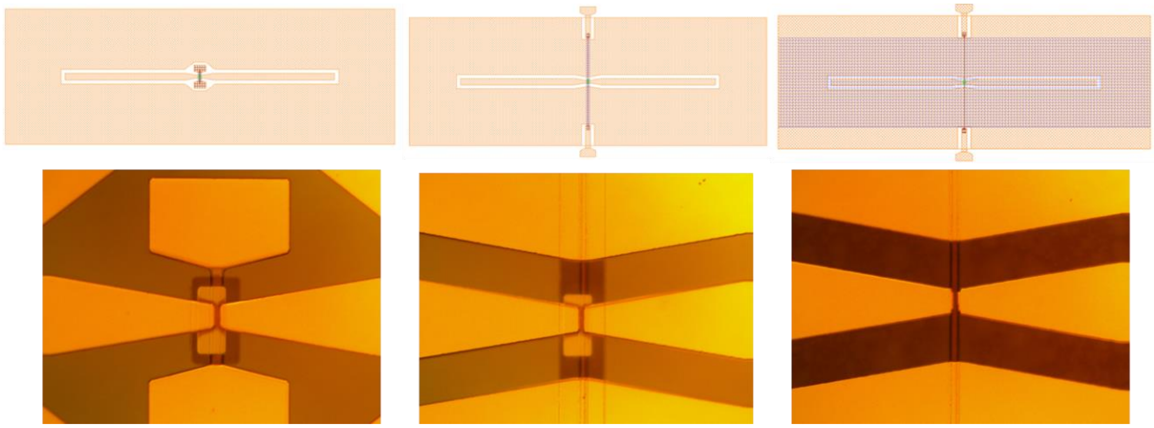

Figure 19. Three new designed switch structures on top and the fabricated results on the bottom.

The first device fabrication was done with a new photoresist (AZ-NLoF 2035) with a higher thickness to lift off thicker metal (Cu/Au) to get closer to needed thickness for skin depth at a lower frequency. This photoresist has not characterized correctly (Under-Exposure) which results in the metal lifted off by RF electrodes. The second Run was finished and tested but a very thin layer of tungsten layer was not etched results in all devices were short-circuited by it. The sputtering and etching process of W were modified after this run to completely etch it with a minimum undercut. The third device run fabricated successfully and tested, the three structures was designed on a new mask and the fabricated results are shown in Figure 19.

## 3.3 Experimental Results

As soon as a fabrication run was completed, the devices were tested using a Cascade Microtech probe station with G-S-G air-coplanar probes. All measurements were conducted using an Agilent performance network analyzer (PNA). At first, the reference standards were tested to verify that the conductor film quality was acceptable by testing the shorted reference. Also, the open reference provides insight into the performance of the silicon substrate and the maximum achievable isolation. This was then followed by the measurement of the PCM switch samples. At first, the switches were measured in the on-state and then biasing was applied.

Figure 20. RF probe setup.

**2016:**

During that test too much current was passed through the NiCr heater and it ended up completely melting the GeTe, which resulted in a catastrophic failure of the device as can be seen in the right image in Figure 21 where the PCM has completely melted. During biasing, the GeTe was observed in a molten state.

This issue is currently being addressed. The isolation of the switch was quite decent, and the result is close to the reference standard, with greater than 25 dB of isolation up to 20 GHz.

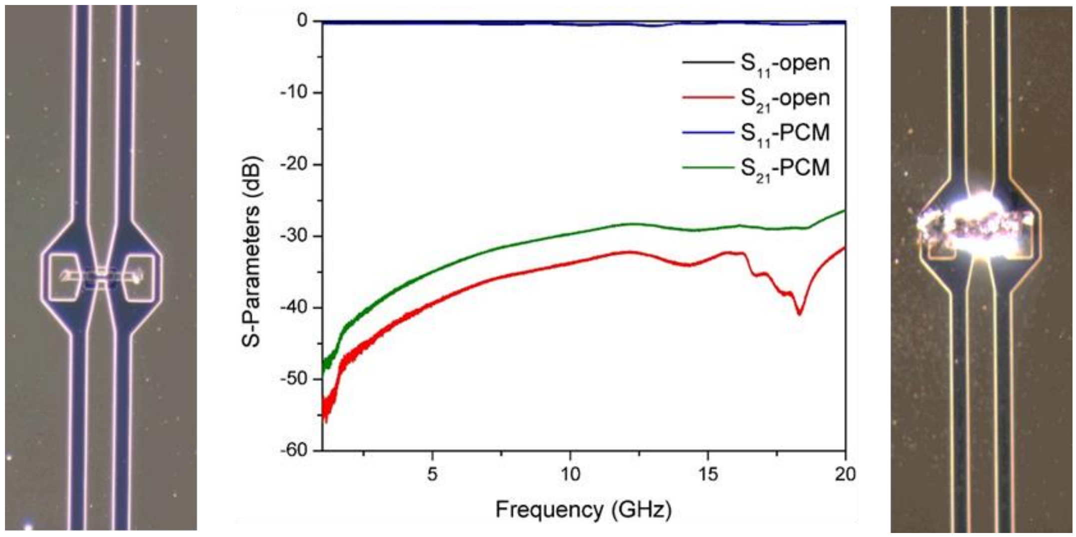


Figure 21. Measured Design 1 PCM sample compared to the open reference in the middle. Design 3 sample before and after direct biasing on the left and on the right, respectively.

## 2017:

The cause for that was the fact that SiO2 had been chosen as the dielectric barrier between the DC and RF. Post analysis revealed that the temperature drop across the SiO2 was a few hundred degrees. The logical solution was to replace the oxide with a good thermal conductor. Aluminum nitride (AlN) was chosen. The AlN was also grown using the PED tool. The AlN film growth was tested by growing the films at a variety of growth conditions, such as temperature, gas pressure, and electron gun properties. All experiments resulted in poor film quality. Since high-quality AlN films were not available, a new design was conceived, one which does not rely on a dielectric barrier. This design is referred to as direct heating, whereas the previous solution is called indirect heating. The first attempt was to simply remove the dielectric layer and build the switches just as before. This resulted in the switch shown on the left in Figure 22. A new circuit for controlling the biasing was created and is shown in Figure 23. Also, in the same figure, the set temperature profiles as well as the achieved profiles are shown for both the on and off switching.

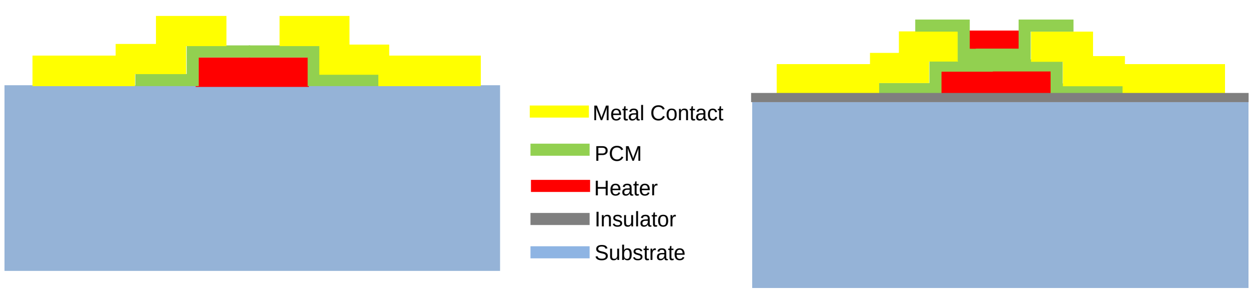


Figure 22. Direct heater cross-sectional views. Design with a bottom heater only on the left and a design with both a top and a bottom heater on the right.

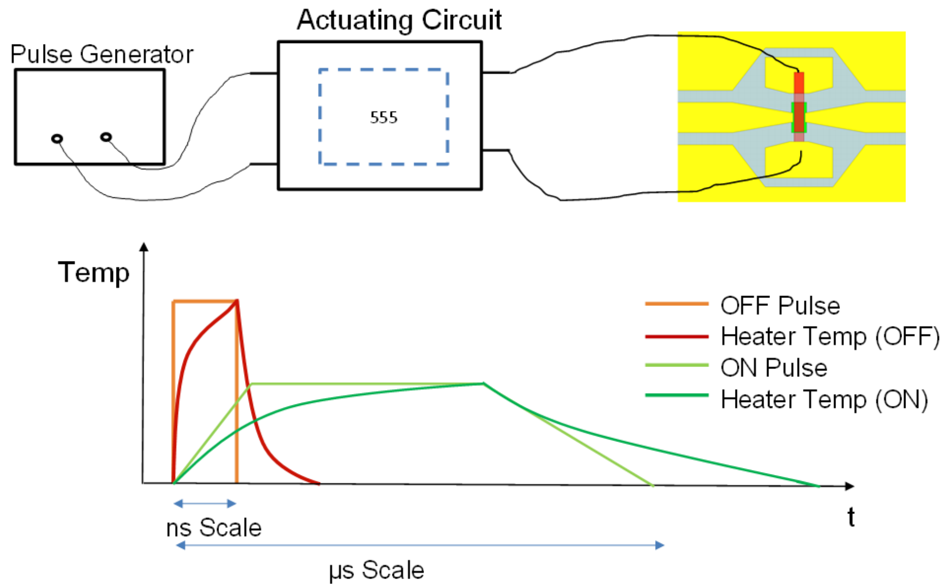


Figure 23. The biasing system concept for PCM switch actuation on top and the set temperature profiles along with the actual profiles are shown on the bottom.

## 2018:

A new circuit for controlling the biasing was created and is shown in Figure 24. Also, in the same figure, the set temperature profiles, as well as the achieved profiles, are shown for both the on and off switching. The measurements of the Indirect-heating switch before applying any pulses shows 2-5 dB insertion loss for frequency above 6 GHz (Figure 25). The switch was considered as ON because of its relatively low insertion loss due to thermal annealing for amorphous deposited GeTe has been done. By applying OFF pulse the insertion loss dropped by 7-10 dB as can be seen in Figure 25. Attempts for turning on the switch was unsuccessful due to the deforming and oxidation of GeTe after melting by OFF pulse.

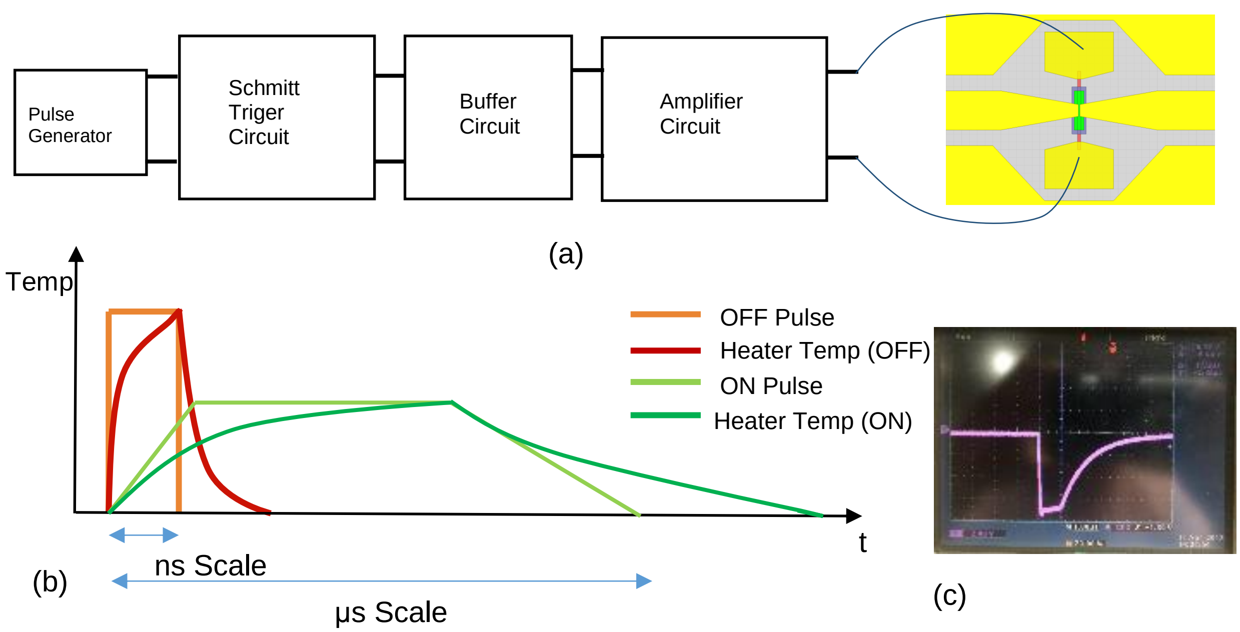


Figure 24. (a) The actuating circuit block diagram, (b) the set temperature profiles along with the actual profiles, and (c) the produced ON pulse.

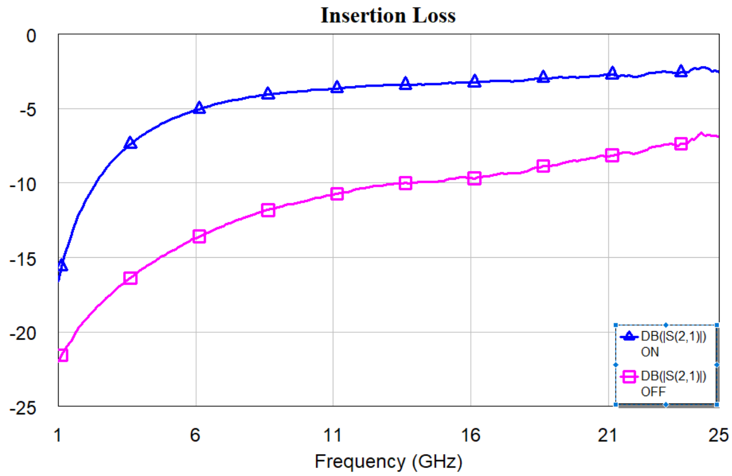


Figure 25. The measured insertion loss of the switch showing signs of phase-change as the switch was biased.

GeTe expanded and oxidized after applying the OFF pulse, which heated it above the melting point and quenching it rapidly to make amorphous GeTe. This can be seen in Figure 26 (b). This problem is due to melting GeTe while it has not protected by a passivation layer and in presence of oxygen ($O_2$).

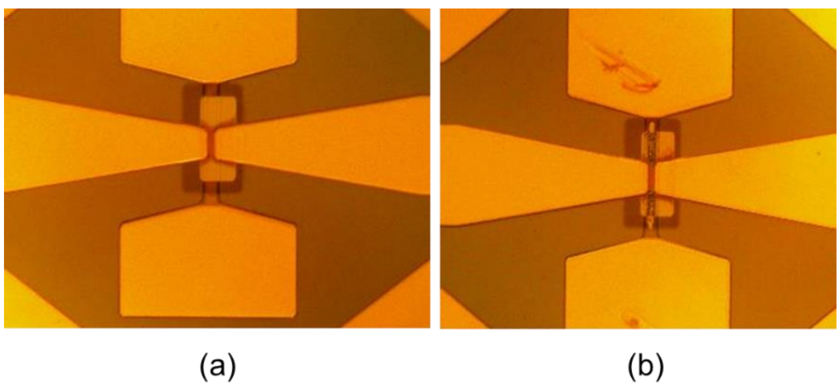


Figure 26. (a) Switch top view before applying OFF pulse, (b) Switch after applying OFF pulse.

## 2019:

To solve this problem, a passivation layer that prevents expanding and oxidation of the GeTe should be added to the structure. A pattern for the passivation layer was designed and a mask ordered. Different materials for this layer were tested. Silicon dioxide ($SiO_2$) and aluminum nitride (AlN) were tested for this purpose. Due to high temperature deposition of $SiO_2$, lift-off is not possible, however, etching is not an option either because of the insulator layer of $SiO_2$, shown in Figure 15. Therefore, AlN is used as the passivation layer. Figure 27 shows the final switch with the GeTe layer covered by AlN to prevent it from oxidation during the thermal activation.

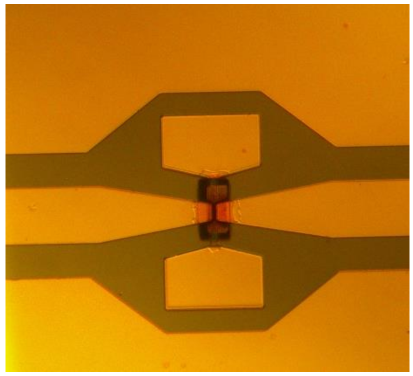

Figure 27. Passivation Layer on top.

## 3.4 LASER-BASED SWITCHING

In order to change the phase of the PCM, thermal cycling is required. The approach being investigated in this project is based on direct laser heating. Figure 28 shows a schematic of the laser setup. There are two 45-degree mirrors redirecting the beam path and a lens to focus the beam. The beam ends on the sample of GeTe which is attached to two DC probes measuring the resistance across it. This setup actively measures resistance of the sample as it is being shot with the laser. The focal point is adjustable by moving the lens further or closer to the sample. The laser being used is an Opt Lasers B445-4000CM. The wavelength of the beam is 445nm and the max power output is 4W. The laser is being pulsed using an Mbed microcontroller. The laser driver utilizes an analog input which grants full control over the output power and pulse width. The mirrors and optics are from Newport. The modular design of the optical system allows for easy adjustment of the beam path and spot size. The Cascade Microtech DC probes are used to measure the resistance across the samples as they are being shot with the laser; the Keithley 2400 is used to actively record this data.

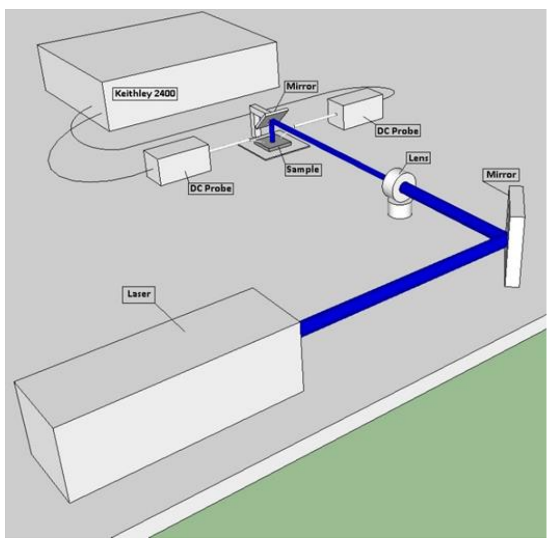


Figure 28. 3D schematic of the laser heating system.

The current status of the laser heating system is that it is fully operational and ongoing tasks include further decreasing the spot size, adding a power calibration module to it, and characterizing the laser heating profile. The last task is being approached both via simulations and direct thermal sensing.

# 4 3D PRINTING OF PCM

The technique used in this portion of the project is being developed on an internally sponsored project where the goal is 3D printing of LTCC materials in a layer-by-layer, additive fashion forming ceramic circuit boards with embedded passives, integrated antennas, and multitier pockets for active circuitry such as high-power transistors and switches. The primary tasks in this project are the development and characterization of printable materials and fabrication processing steps needed to demonstrate the feasibility of rapid prototyping LTCC circuit boards. The printable LTCC dielectric suspension consists three ingredients: Heraeus X200 ceramic LTCC powder, Sartomer SR238 monomer, and Variquat CC-55 dispersant.

In this project part of the project the goal is to print a suspension loaded with PCM as part of the 3D printed LTCC process currently being developed at OU. Adding this material will allow direct printing of new devices such as switches and varactors. Figure 29 shows an RF switch that will be realized using the inclusion of PCM printing into the LTCC process [1]. The switch design will be the same as was designed for the electrical characterization task.

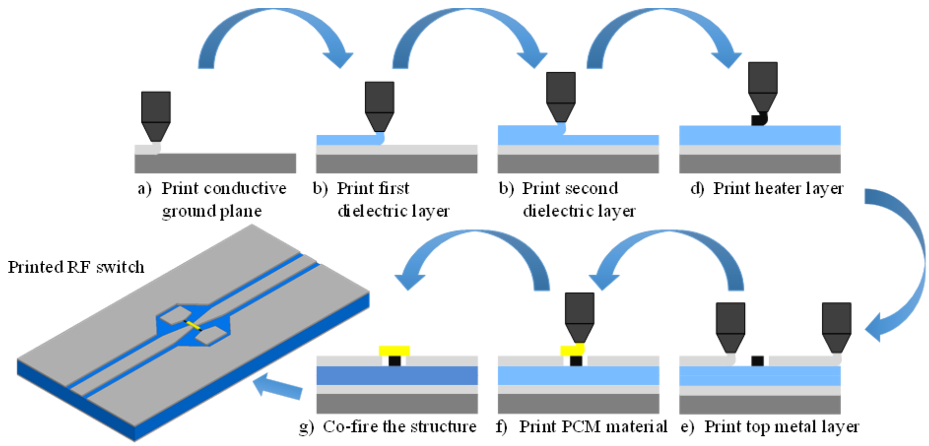


Figure 29. Conceptual example of multi-material printing. Four different materials are used to print a PCM-based RF switch (not drawn to scale).

The first step was to procure finely ground GeTe powder, again from American elements, and mix it with the same monomer as was used for the printed dielectric material. The solution was then dispensed between two fired silver traces on an aluminum oxide substrate. This sample was subjected to the LTCC firing profile that is being used for the 3D printed LTCC. After firing, the dispensed GeTe pattern had greatly diminished in size and there was not much material apparently left behind. This may be due to the fact that the melting temperature of GeTe is lower than the firing temperature of LTCC and thus the material may have been thermally evaporated. A new slurry mixture that can be fired at lower temperatures is needed. Heraeus has an LTCC system that is fired at temperatures closer to 500°C is a good candidate for continuing this work.

A DURIP proposal was submitted for the acquisition of an nScrypt 3D printers with four dispensing pumps. This equipment is necessary in order to print accurate traces and patterns for this task. Early experimental printing was done using a home-made printer with only the x- and y-axes computer controlled. The z-axis was manually controlled and that resulted in non-uniform printing. The new printer allows for very accurate printing of traces down to few tens of micrometers. This task is ongoing and currently LTCC substrates with conductive pastes are being co-printed and co-fired. The result of this portion of the work will be published this year.

# 5 SUMMARY OF ACCOMPLISHMENTS

The following accomplishments were completed during the performance period of the project.

- Germanium telluride (GeTe) phase-changing material (PCM) was grown for the first time using a pulsed electron deposition (PED) tool.
  - Films of various thicknesses demonstrated.
  - Growth conditions determined.
  - Growth rates characterized.
  - Film quality investigated.
  - A detailed study on the growth of GeTe using PED published in a journal [4]. Second paper in preparation with details on activation of PED-grown GeTe.

- The PED tool was reworked to improve the accuracy and control of the deposition.
  - Sample holder extension designed and fabricated.
  - Crystal monitoring added for in-situ growth monitoring.
  - A shutter was incorporated in order to allow for target cleaning via material pre-deposition.
  - Butterfly valve replaced with turbo valve to give better control on pressure.
  - A shutter was incorporated in order to allow for target cleaning via material pre-deposition.
  - Sputtering system added to PED chamber.

- Multiple revisions of GeTe-based RF switches were designed and fabricated.
  - The RF gap was reduced to the minimum size that can be fabricated in the University of Oklahoma cleanroom.
  - Different passivating materials were investigated. Necessary to prevent oxidation of the GeTe material.

- Materials acquired for 3D printing of PCM-based slurry.
  - Formation of PCM-based slurry investigated.
  - Slurry co-fired on a ceramic substrate.
  - A professional 3D printer, that is ideal for this type of printing, was acquired through a DURIP.

- A tunable filter design incorporating the GeTe PCM switches was conceived.
  - Full-wave electromagnetics simulation model of a new tunable filter with PCM switches was demonstrated.

- Dielectric and heater layers' materials were deposited and shaped.
  - Sputtering AlN with AlN and Al target tested and characterized.
  - E-beam and sputtering deposition of Mo and W were done to find the best deposition method.
  - Tungsten etchant was investigated. This included the determination of the proper chemical mixing ratios and the resulting etch rates.

- PCM-based RF switches designed and fabricated.
  - several designs were investigated and two of them selected for fabrication.
  - Microfabrication processing optimized for the switch geometries.
  - Direct and indirect heating switches designed, fabricated, and tested.
  - The accurate pulse generating circuit was designed, made and tested.
  - Switches were tested, and its problem was found.

# 6 REFERENCES


[1] H. Sigmarsson, "Reconfigurable, High-Frequency Circuit Components using Phase Change Materials," Annual Project Report Apr. 2016.

[2] H. Sigmarsson, "Reconfigurable, High-Frequency Circuit Components using Phase Change Materials," Annual Project Report Apr. 2017.

[3] H. Sigmarsson, "Reconfigurable, High-Frequency Circuit Components using Phase Change Materials," Annual Project Report Apr. 2018.

[4] N. Bathaei, B. Weng, and H. H. Sigmarsson, "Growth study of GeTe phase change material using pulsed electron-beam deposition," *Materials Science in Semiconductor Processing*, vol. 96, pp. 73-77, Feb. 2019.